Biotribology 22 (2020) 100125

Contents lists available at ScienceDirect

Biotribology

journal homepage: www.elsevier.com/locate/biotri

Hydrogel compression and polymer osmotic pressure

Abir Bhattacharyya[a], Chris O'Bryan[b], Yongliang Ni[c], Cameron D. Morley[c], Curtis R. Taylor[c], Thomas E. Angelini[c,*]

[a] Department of Metallurgical and Materials Engineering, Indian Institute of Technology, Jodhpur, Karwar, Rajasthan 342037, India
[b] Department of Chemical and Biomolecular Engineering, University of Pennsylvania, Philadelphia 19104, USA
[c] Department of Mechanical and Aerospace Engineering, University of Florida, Gainesville 32611, USA

ARTICLE INFO

Keywords:
Soft matter
Osmotic pressure
Indentation
Contact mechanics
Hydrogel

ABSTRACT

Controlling the elastic modulus of simple synthetic hydrogels like polyacrylamide is essential to their use in many areas of biotechnology, including tissue engineering, medical device development, and drug delivery applications. Indentation-based methods for measuring hydrogel elastic moduli are preferred over measurements in shear rheometers or tensile testing instruments when the freedom to choose sample volume and shape are restricted; contact lenses represent such an example. It is often believed that the local application of indentation loads will volumetrically compress hydrogels, increasing the sample's polymer concentration even when the applied pressure is less than the hydrogel's osmotic pressure. Here, we test this idea by volumetrically compressing polyacrylamide hydrogels of different compositions while measuring the degree of compression with increasing applied pressure. Our results reveal that at applied pressures below the hydrogel osmotic pressure, the gels exhibit only marginal compression, while above the osmotic pressure the gels compress as predicted by classical polymer physics theory. Combining measurements of osmotic pressure and polymer mesh size, we determine the scaling relationships between hydrogel composition, mesh size, and osmotic pressure. By demonstrating agreement between experiment and theory, we use our measurements to determine the Kuhn length of the individual polymer chains constituting the hydrogels.

1. Introduction

The ease with which hydrogels can be synthesized to have elastic moduli comparable to that of living tissue makes them useful in numerous biologically related applications such as scaffolds for tissue engineering and medical devices like contact lenses [1–5]. While a diversity of different kinds of hydrogel exist, varying in nanostructure, microstructure, polymer solvation strength, elastic modulus, and fluid permeability [6–9], the most basic and fundamental starting point for understanding hydrogel properties is the fully swollen network of permanently crosslinked flexible polymers in a good solvent [10]. Our ability to leverage simple polymer physics to understand the behaviors of such “ideal” hydrogels like polyacrylamide (pAAm) has made them useful in biotribological studies [3,11], as all their material and transport properties are governed by the correlation length of their thermally fluctuating polymer chains [12,13]. This correlation length, known as the mesh size, ξ, is typically on the order of nanometers. While these ideal hydrogels represent a powerful experimental platform for fundamental study, in addition to their usefulness in applications, their ability to mimic tissue is limited; biological tissues contain microscale pores, by contrast, and can be potentially described as water permeated cellular solids [14]. These differences between ideal hydrogels and tissues in terms of their micro- and nano-structure and the correspondingly different role of entropy in determining their material properties may lead to contrasting mechanical response to compressive loading. It was recently demonstrated that pAAm hydrogels do not compress under local pressure applied by indentation loading, and globally compress only when the applied pressure exceeds the osmotic pressure, Π, of the hydrogel network [15]. However, only one composition of the hydrogel was tested in this study. To firmly establish that the change in compressibility is associated with osmotic pressure, a systematic investigation needs to be performed for various hydrogel compositions and the scaling relationships between Π, ξ, and polymer concentration, c, must be tested. A direct comparison between empirical measurements of these scaling relations and basic polymer physics predictions is necessary to provide new interpretations of the responses of flexible semi-dilute hydrogels to applied loads, most notably those measured under local contact pressures generated in micro-

* Corresponding author.
E-mail address: t.e.angelini@ufl.edu (T.E. Angelini).

https://doi.org/10.1016/j.biotri.2020.100125
Received 29 August 2019; Received in revised form 3 March 2020; Accepted 9 March 2020
Available online 11 March 2020

and nano-indentation tests in which it is often believed that hydrogels volumetrically compress.

In this work, we evaluate the role of osmotic pressure in hydrogel compression response and investigate the scaling relationships between Π, ξ, and c. The concentration and mesh size of the hydrogels are varied by changing the concentrations of monomers and chemical cross-links. The Π values measured from uniaxial compression experiments are correlated with the measured mesh sizes of the swelled hydrogels to determine the scaling relationships. Finally, the experimentally obtained relationships are compared with polymer physics scaling laws for flexible semi-dilute polymer networks.

2. Materials and Methods

2.1. Hydrogel Formulation

Four different concentrations (c_i= 3.75 wt%, 5 wt%, 7.5 wt%, and 10 wt%) of pAAm hydrogel were synthesized by mixing acrylamide (AAm) monomer, *N*, *N′*-methylenebisacrylamide (MBAm) cross-linker, 0.15 wt% ammonium persulfate (APS) initiator, and 0.15 wt% tetramethylethylenediamide (TEMED) catalyst, in ultrapure water. The monomer to cross-linker ratio was always kept same for all pAAm compositions. After pipet mixing in a glass vial, the gel was cast within a mold, cured, removed from the mold, swelled to equilibrium in ultrapure water before mechanical testing and characterization.

2.2. Compression Testing

For compression testing, a circular punch with 20 mm internal diameter was used to cut disks from the 0.5 mm thick swollen hydrogel slabs. Force-controlled quasi-static compression tests were conducted on the disk-shaped hydrogel samples in rheometers using plate-on-plate geometry (Anton Paar MCR 702 and Malvern Kinexus Pro). The average roughness of the plates is approximately 5 μm [15]. Stepped loads were applied on hydrogel disks and each load was held for 90 min to allow equilibration of the gel. Excess water was wicked around the plates and the gels to prevent evaporation of water from hydrogels during the test. A temperature of 25 °C was maintained throughout the tests.

2.3. Small Angle X-ray Scattering

Small angle x-ray scattering experiments (SAXS) were conducted on pAAm hydrogels in Bruker NANOSTAR SAXS system to measure the nanoscale mesh sizes of each gel composition. The hydrogel samples were prepared by pipetting the gel mixture into amorphous quartz capillary tubes of 1.5 mm diameter and 10 μm wall thickness before polymerization. The uncured hydrogels within the capillary tubes were centrifuged at a low speed to collect all materials at the bottom of the capillaries. The hydrogels were then allowed to cure and subsequently were equilibrated with equal volumes of 100 mM CsCl solution for 48 h to achieve a swollen state of the gels. The CsCl improves the *Z*-contrast between the polymer and the solvent, as previously shown [11]. The quartz capillaries were flame sealed to prevent evaporation of water during the SAXS experiments. The SAXS data were collected for 18 h per sample on a 2-dimensional (2D) wire detector with 1024 ×1024 pixels and were analyzed to estimate the corresponding mesh size.

3. Results and Discussion

Uniaxial compression experiments were conducted on swollen pAAm hydrogels to determine the polymer osmotic pressure, Π^*, corresponding to the swollen polymer concentration, c^*. According to the well-known c^*theorem [10], the polymer concentration, c, of the fully swollen cross-linked gels is the same as the overlap concentration of a corresponding solution of un-crosslinked polymers, $c*$, and the corresponding osmotic pressure in the gels is defined as Π^*(Fig. 1(c)). The c^* theorem is typically framed within an infinite system, connecting the properties of semi-dilute polymer solutions to those of fully swollen crosslinked gels. We find it useful to re-cast the c^* theorem in an experimental context, in which the polymers are contained within a semi-permeable vessel that allows only water transfer, depicted by the dashed lines in Fig. 1. In this context, the polymers in solution randomly collide with the semi-permeable walls, exerting a pressure equal to their own osmotic pressure, Π, and balanced in equilibrium by an externally applied pressure outside the vessel, *P*, assuming the vessel can change size. For dilute solutions up to the semi-dilute limit, the osmotic pressure follows the ideal gas law, $\Pi \approx ck_BT$, where $k_B$is Boltzmann's constant, and T is the temperature in Kelvin, and c is the number of chains per-unit-volume (Figs. 1(a-b)). While the polymer chains are far apart for dilute solutions ($c < c*$), by increasing *P*, the individual polymers can be pushed together until the polymer chains just begin to overlap reaching the semi-dilute concentration in which $c = c*$ and $\Pi = \Pi^* = P$ (Figs. 1a, b). If the polymers are then crosslinked at c^* with optimal crosslinking density, a fully swollen network is formed (Fig. 1c). At this point, if the barrier was removed, the gel would not swell, while putting the barrier back in place and applying lower applied pressures, $P < \Pi^*$, the gel should not compress. By contrast, further increasing *P* above Π^*, the gel should compress, driving water out of the gel through the semi-permeable container (Fig. 1d), as previously observed [15]. While this picture represents the ideal case, and different types of gel systems exhibit syneresis under externally applied pressure [16,17], here we aim to test how well the predicted the scaling between*P*, Π, c, and ξ compare with the simple predictions of classical polymer physics.

3.1. Hydrogel Equilibration and Compression Tests

To determine the degree of swelling of samples and to ensure they approach $c^*$for later testing, 12.7 mm long cylindrical specimens with 12.7 mm diameter are prepared by casting the hydrogels within glass tubes. The specimens are removed and fully submerged in ultrapure water. Swelling curves are created by measuring the mass of each specimen at numerous time-points, wicking away excess water before weighing. The change in mass relative to the initial mass of the gel is computed, given by $(m_t - m_i)/m_i$, where m_i and m_t are initial mass and mass at any arbitrary time, t. We find that for all samples tested, swelling reaches a plateau after approximately 120 h, while 90% of the fully swollen volume is achieved within 48 h (Fig. 2a). To avoid potential problems associated with long swelling times like contamination and sample degradation, we choose to analyze samples at the 90% swelling, 48 h mark. The sample volume at this time-point, V^*, is used to estimate the equilibrium concentration of the gel using a conservation of mass relationship, given by $c^* = c_iV_i/V^*$, where c_i and V_i are the polymer concentration and sample volume as prepared before swelling. Here, we note that the concentrations used in different theoretical models and in different experiments often have different units. For example, the ideal gas law describing the osmotic pressure of a dilute polymer solution is often cast in units of polymer chains per unit volume. By contrast, in the Flory-DeGennes theory of hydrogels described below, the concentration units are Kuhn lengths per unit volume. In our experiments, we find it the most accessible units of concentration for sample preparation and data analysis to be weight percent (mass of monomers per unit mass of sample multiplied by 100). These different metrics of concentration can be interchanged when the relevant microscopic parameters are known, such as the Kuhn length, the chain length, and the monomer mass. Similarly, the relationship between polymer mesh-size and concentration can be altered by using different concentration units. Thus, the scaling relationships hold for any of these different types of concentration, allowing scaling laws to be tested up to unknown multiplicative coefficients. We therefore use units of weight percent throughout the experimental part of this manuscript and convert to units consistent with theory later when we perform more

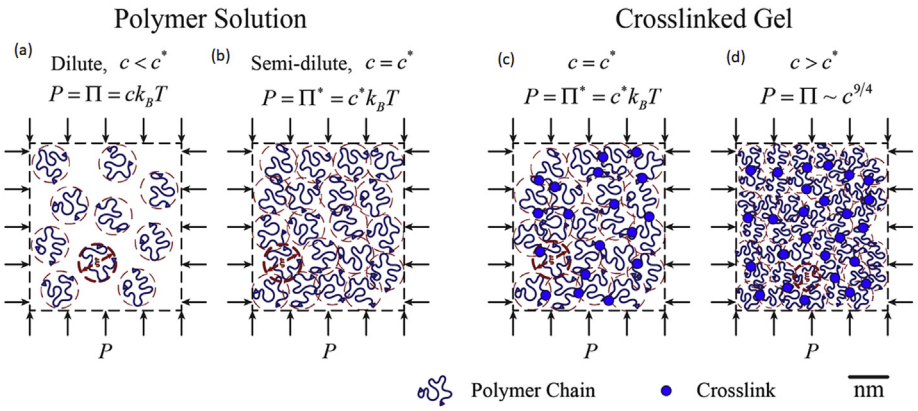

Fig. 1. Schematics explaining the concept of osmotic pressure of dilute and semi-dilute polymer solution (a-b), and of crosslinked gel (c-d). The osmotic pressure of dilute and semi-dilute polymer solution and gel follows ideal gas law. The concentration of the semi-dilute solution and gel reaches c^* at the fully swelled state. Beyond c^*, the osmotic pressure of semi-dilute solution and gel follows $c^{9/4}$ scaling law. The diameter of the spherical correlation volume in polymer solution or gel is its mesh size (ξ).

detailed analysis.

To determine the role of osmotic pressure in hydrogel compression, and subsequently measure $\Pi^*$for each hydrogel composition, swollen hydrogel disks of diameter d_o = 20mm and thickness h_o = 0.5mm are placed between roughened parallel plates in a rheometer. The disks are subjected to uniaxial compression loading (Fig. 2b). The roughened plates prevent the gels' tendency to slip during the application of compressive loads, ensuring that volume changes are proportional to thickness changes; tests using smooth plates consistently exhibited radial expansion, leading us to use roughened plates. Discrete compressive loads of increasing magnitude are applied sequentially to the hydrogel disks. In each load step, the force is held constant for 90 min and the gap between the parallel plates is recorded by the rheometer as a function of time. Upon visual inspection, we found no lateral expansion of the hydrogel disks during any of the compression tests (Fig. 2c). Thus, the lateral strain is assumed to be zero, given the low aspect ratio of the disk-shaped hydrogel samples. The longitudinal strains, given by given by$\varepsilon = \delta h/h_o$, are determined from the measured gap between the parallel plates, averaged over the final 300 s of each loading step, during which the gap was observed to remain constant. We plot the strains versus applied pressure,P, for all four pAAm compositions in Fig. 2d. Two distinct regimes of compressive response are observed with a clear transition between the two trends. The experimental data points in the two regimes are fit with power laws, $\varepsilon = KP^n$, and the strain and pressure intersections of the fitted lines are defined as transition strains and transition pressures for each sample composition. For applied pressure lower than the transition pressure, the increase in strain with applied pressure is only very small, while beyond the transition pressure the strain increases rapidly with increasing applied pressure, corresponding to a regime in which sample volume strongly decreases with increase applied pressure. The systematic increase in transition pressure with increasing polymer concentration suggests that this transition pressure may be the semi-dilute osmotic pressure, Π^*, of the hydrogel at c^*.

3.2. Polymer Mesh Size Measurements for Predicting Π^*

One way to test whether the transition pressure observed above is the semi-dilute osmotic pressure, is to measure the polymer mesh-size, ξ, in fully swollen gels and employ the relationship between Π and ξ predicted from basic polymer physics, given by $\Pi = k_BT/\xi^3$ [10,18]. We therefore measure ξ and compute a predicted semi-dilute osmotic pressure, Π^*_{pred}, then compare it to the experimental transition pressure, Π^*_{meas}, measured through compression tests. We measure hydrogel sample mesh-sizes using small angle x-ray scattering (SAXS). In SAXS, the scattered x-ray intensity is measured as a function of a scattering angle relative to the direct beam, 2θ. Traditionally, this scattering angle is converted to a scattering wave-vector, q, given by $q = (4\pi/\lambda)\sin(\theta)$, where λ is the X-ray wavelength and θ is half the scattering angle. The 2D scattering profiles are integrated around the direct beam, along the azimuthal angle, to produce 1D intensity curves. To determine the hydrogel mesh-size, ξ, the intensity profiles are fit with a Lorentzian line-shape given by $S(q) = A_0 + \frac{A\xi}{(q\xi)^2+1}$, where A_0 and A are instrument-dependent constants. The scattering intensity vs q profile of 5 wt % hydrogel along with a fitted Lorentzian curve are shown in Fig. 3a as an example. The rapid rise in scattered intensity at low q arises from scattered intensity around the instrument beam-stop and are ignored in the fitting process.

By plotting the measured mesh-sizes as a function of the corresponding fully swollen polymer concentrations in each hydrogel, we find that the mesh size decreases with increasing polymer concentration (Fig. 3b). In fully swollen gels, the mesh size, ξ, is predicted to fall with increasing polymer concentration following a power law, given by $c^{-3/4}$.

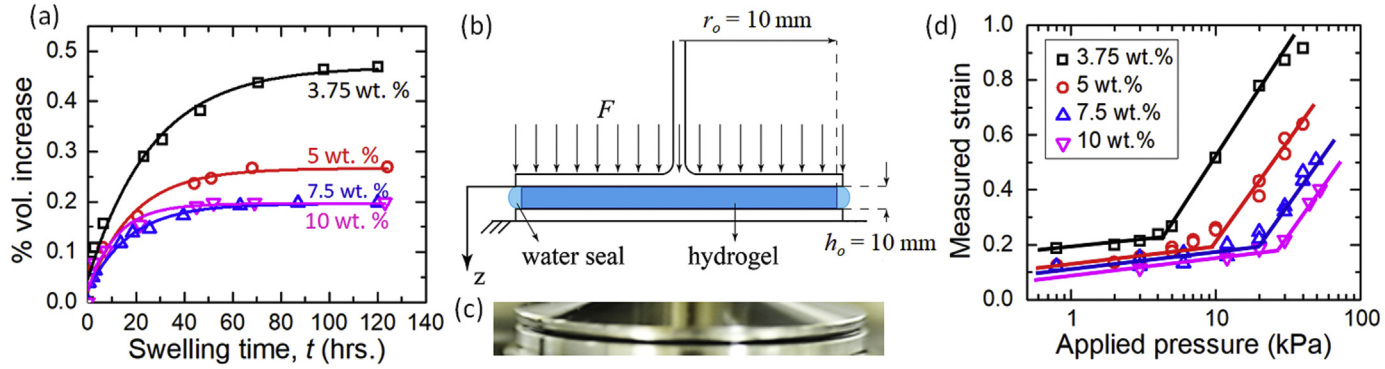

Fig. 2. (a) Swelling characteristics of four pAAm gel compositions as a function of equilibration time in water. (b) Schematic of compression test conducted on fully swelled gels between roughened parallel plates in a rheometer. (c) Image of a hydrogel disk subjected to compression shows no lateral expansion. (d) Compressive strain vs applied pressure responses for the same pAAm compositions showing higher transition pressures with increasing polymer concentration.

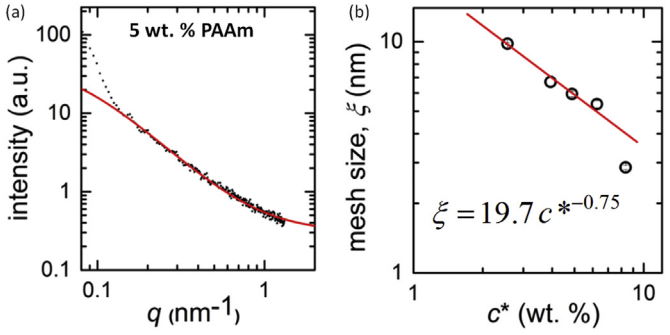

Fig. 3. (a) Small angle x-ray scattering spectra for three pAAm gel concentrations. (b) Mesh size, ξ as a function of c^*. Note that $\xi \sim (c^*)^{-0.75}$ at low concentrations.

Fitting this power law to the hydrogel compositions at the low end of concentration, we find $\xi = 19.7c^{*-3/4}$. We quantitatively analyze the pre-factor of 19.7 later. The data-point corresponding to the highest concentration sample deviates from this trend, which we attribute to the possibility that the sample is in the concentrated regime, where the polymers no longer behave as totally flexible.

3.3. Comparing Structural and Mechanical Measurements Using Polymer Physics Scaling Laws

To test whether the structural measurements of polymer mesh-size are consistent with the mechanical measurements of the cross-over pressure, we predict the osmotic pressure from measurements of ξ, using the relationship $\Pi^*_{pred} = k_B T/\xi^3$. For samples measured using both techniques (3.75–7.5 wt%), plotting Π^*_{pred} versus the measured cross-over pressure, Π^*_{meas}, reveals a linear correlation (Fig. 4a). A best-fit line through these data-points shows that the trend lays within a factor of less than 0.67 from the perfect prediction of $\Pi^*_{pred} = \Pi^*_{meas}$. This discrepancy may arise from the known micro-scale heterogeneities found in hydrogels like pAAm, which are likely to contribute to their macroscopic material properties. Alternatively, the discrepancy may arise from swelling the x-ray samples in glass capillaries; the factor of 0.67 would correspond to the samples prepared for x-ray measurements swelling by 84% relative to the unconfined gels that were prepared for mechanical testing. While the samples were equilibrated for the same periods of time and the gels in the x-ray capillaries may have continued to swell throughout the measurements, it is reasonable to expect that the confined gels would swell less. Overall, given the idealized nature of the scaling laws predicted from simple polymer physics, we believe this close agreement indicates that the transition pressure measured in mechanical compression tests is likely the osmotic pressure arising from the dynamic, nano-scale, polymer structure reflected in the polymer

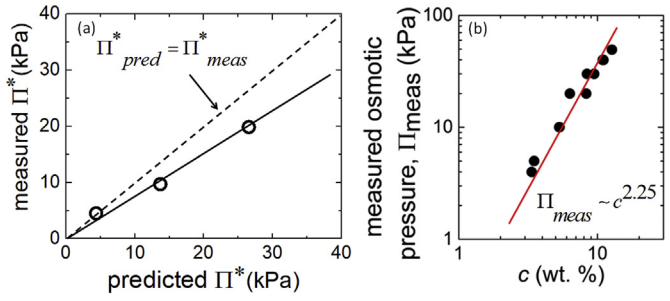

Fig. 4. (a) Comparison of measured transition pressure with osmotic pressure predicted from the measured mesh sizes. A best-fit line through these data-points (solid) shows that the trend lays within a factor of less than 0.67 from the perfect prediction of $\Pi^*_{pred} = \Pi^*_{meas}$. (b) A semi-dilute concentration region showing $\Pi \sim c^{2.25}$ scaling beyond c^*.

mesh size, measured with SAXS. The measured and predicted Π^*values of the hydrogels are tabulated in Table 1 along with their respective measured mesh-sizes. The modulus values presented here match well with the literature.

Given the level of agreement between Π^*_{meas} and Π^*_{pred}, we extend our analysis to the compressed regime of our uniaxial mechanical tests, in which $P > \Pi^*$. In these mechanical tests, as the hydrogel compresses, the polymer concentration is proportional to the thickness reduction of the hydrogel disc and can be determined from the strain, γ, according to $c = c^*/(1 - \gamma)$. In Fig. 4b we plot the applied pressure, Π_{meas}, beyond the transition pressure,Π^*, versus the instantaneous concentration, c. We find that these data also follow the $\Pi \sim c^{9/4}$scaling law for semi-dilute networks. A best-fit curve of this power law shows $\Pi = 0.21c^{9/4}$ (Fig. 4b). Comparing this scaling law with the osmotic pressure predicted from $\Pi = k_B T/\xi^3$, we find that the two trends agree within a factor of 2.6, where $\xi \approx 19.7c^{-3/4}$is used as an empirically determined map between c and ξ. Once again, given the approximate nature of the basic polymer physics predictions, we believe our mechanical tests dominantly measure the polymer osmotic pressure, generated by the thermal fluctuations of polymers resisting compression.

To further test our measurements using fundamental polymer physics, we employ the full relation between osmotic pressure and polymer concentration based on Flory's and DeGennes' theories, given by $\Pi = k_B T c^{9/4} V^{3/4} a^{3/2} = k_B T/\xi^3$ [10], where $V$is the excluded volume parameter defined as $V = a^3(1 - 2\chi)$, a is the Kuhn length of each monomer of a polymer chain containing N monomer segments, and χ is the Flory interaction parameter [10]. We note that this formula for Π is identical to the scaling law describing the hydrogel elastic modulus; the thermal fluctuations underlying the osmotic pressure in these types of hydrogels also give rise to their elastic moduli, which is often called "entropic elasticity," as the flexible chains have no internal elasticity that resists deformations over length scales exceeding the Kuhn length. After substituting the empirical result $\xi \approx 19.7c^{-3/4}$, we find that for our system, $V$and a are related to each other by a simple equation $V^{-1/4}a^{-1/2} = 19.7$. Assuming $\chi = 0$ for athermal solvents in semi-dilute concentration regime, find the Kuhn length to be 0.41 nm. Similarly, the Kuhn length can also be predicted from our other empirical result $\Pi = 0.21c^{9/4}$. From this measurement we find the Kuhn length to be 0.31 *nm*. Based on chemical formula of acrylamide, one monomer contains two C−C bonds with bond length of 0.154 nm. Therefore, our two different measurement routes indicate that one Kuhn length consists of approximately 1–2 monomers, as is expected for a flexible polymer like pAAm [19,20].

The relationship between Kuhn length and monomer length can be used to estimate the number of Kuhn length segments (N) in a polymer mesh for semi-dilute pAAm gels. In the theories employed here, the concentration c is defined as the ratio between the number of Kuhn lengths per unit volume within defined by the polymer mesh-size. For a semi-dilute solution, this concentration is given by $c = \frac{N}{\xi^3}$. This concentration can be equated to the experimentally measured c^* from swelling measurements to estimate Naccording to $100 \times \frac{mNM_w}{N_A \xi^3} = c^*$, where c^* is measured in wt%, m is the number of monomers in one Kuhn length, M_w is the molecular weight of the AAm monomer (71.08 g/mol), and N_A is Avogadro's number. For $m = 1$, the estimated value of Nvaries between 16 and 204 for c^*within the range we experimentally investigated, 2.56–8.34 wt%. Similarly, for $m = 2$, Nvaries between 8 and 102 for the same range of c^*. The decreasing numbers of Kuhn lengths per mesh with increasing monomer concentration is consistent with the observed trend in the mesh-size versus monomer concentration; the reduction of N below 10 as c^* approaches 10% is consistent with our observations of the breakdown of predictable behavior at higher pAAm concentrations.

Table 1
Polymer composition and mesh size along with predicted and measured osmotic pressure of pAAm hydrogels.

Polymer wt%	Crosslinker wt%	c^* (wt%)	Mesh size, ξ (nm)	Predicted osmotic pressure, Π_{pred} (kPa)	Measured osmotic pressure, Π_{meas} (kPa)
3.75	0.15	2.56	9.8	4.37	4.5
5.0	0.2	3.94	6.7	13.7	9.8
7.5	0.3	6.26	5.37	26.6	19.85
10	0.4	8.34	2.86	176	28

4. Conclusion

The simple picture of ideal hydrogels painted in DeGennes' famous text [10], based on the connection between gels and polymer solutions at c^*, suggests that these hydrogels should not compress upon the application of external pressure at levels less than their own internal osmotic pressure, Π^*. Testing this idea is critical for correctly interpreting surface contact measurements of such hydrogels, in which potential syneresis could alter both normally directed contact mechanics and interfacial lubrication. Direct observation of the region under an indenting instrument previously showed no indication of polymer compression and syneresis, but the compressibility of these ideal hydrogels was not investigated systematically [15]. The results reported here support the previous conclusion that during indentation tests, these ideal hydrogels do not significantly change volume when applied contact pressures are less than their own internal osmotic pressures. Moreover, the scaling laws of basic polymer physics quantitatively capture the several different measurements described here.

The notion that these ideal hydrogels made from flexible polymers at concentrations near c^* should not compress under infinitesimal levels of applied pressure is counterintuitive from a perspective of equilibrium; a gel that is fully swollen must be under a balance of counteracting forces, and tipping this balance should cause a change in polymer concentration. However, from our understanding of the c^* theorem, the underlying mechanism of the apparent incompressibility is the one main difference between polymer solutions and hydrogels at the overlap concentration: the infinitely rigid crosslinks. If a polymer solution in a semipermeable container is concentrated to c^* until a pressure of Π^* is reached, and then crosslinks are added at the ideal concentration, these crosslinks will hold the polymers together and counteract their outward pressure, reducing the pressure on the container walls to 0. If then additional pressure is applied to the newly formed hydrogel, we expect that the tension in the rigid crosslinks will be reduced without significantly compressing the gel until Π^* is once again reached, since Π^* is the pressure required to begin concentrating the polymers once again. While this explanation is speculative and requires further experimental evidence to prove, it relies on the biggest difference between polymer solutions and hydrogels at c^*: extremely stiff chemical bonds of the crosslinks.

An outstanding aspect of our results is the apparent compression of the gels up to 10–20% strain in the limit of zero applied pressure. So far, we have attributed this to the roughness of the plates used in the experiments. However, if these measurements are not dominated by such artifacts, this regime of lower compressibility at applied pressures below Π^* may reflect a fundamental property of hydrogels that needs further investigation. Additionally, “non-ideal” aspects of pAAm hydrogels that allow for syneresis at low applied pressures, potentially associated with large-scale heterogeneities in gel structure, remain to be ruled out. Yet even if this effect is an experimental artifact, it will be interesting in the future to directly observe whether localized indentation tests at high pressures exhibit polymer compression; we expect our results to inform contact mechanics measurements of polymer systems under focused applied pressure where polymer concentration may locally rise when using small radius indenter tips or large normal-load levels [21,22]. We also believe it will be important to contrast the results reported here with compression tests of hydrogels having extremely different architectures from those of “ideal” pAAm gels. For example, in vitro collagen networks typically have micron-scale mesh-sizes and the fibers between branches in the network are somewhere in the semi-flexible to rigid regimes. In these cases, the gels may respond to compressive forces in a manner closer to that of cellular solids than that of pAAm hydrogels, requiring different interpretations from the one presented here.

Acknowledgements

The authors thank Anton Paar for the use of the Anton Paar 702 rheometer through their VIP academic research program. Funding for this work was provided by Alcon Laboratories.

Declaration of Competing Interests

The authors have no conflicts of interest to declare.

References

[1] N.A. Peppas, et al., Hydrogels in pharmaceutical formulations, Eur. J. Pharm. Biopharm. 50 (1) (2000) 27–46.
[2] C.M. Kirschner, K.S. Anseth, Hydrogels in healthcare: from static to dynamic material microenvironments, Acta Mater. 61 (3) (2013) 931–944.
[3] A.A. Pitenis, et al., Corneal cell friction: survival, lubricity, tear films, and mucin production over extended duration in vitro studies, Biotribology 11 (2017) 77–83.
[4] J.A. Hubbell, Synthetic biodegradable polymers for tissue engineering and drug delivery, Curr. Opinion Solid State Mater. Sci. 3 (3) (1998) 246–251.
[5] B.-S. Kim, et al., Cyclic mechanical strain regulates the development of engineered smooth muscle tissue, Nat. Biotechnol. 17 (1999) 979.
[6] E.M. Ahmed, Hydrogel: preparation, characterization, and applications: a review, J. Adv. Res. 6 (2) (2015) 105–121.
[7] E. Caló, V.V. Khutoryanskiy, Biomedical applications of hydrogels: a review of patents and commercial products, Eur. Polym. J. 65 (2015) 252–267.
[8] A.S. Hoffman, Hydrogels for biomedical applications, Adv. Drug Deliv. Rev. 64 (2012) 18–23.
[9] A.M. Mathur, S.K. Moorjani, A.B. Scranton, Methods for synthesis of hydrogel networks: a review, J. Macromol. Sci. Part C 36 (2) (1996) 405–430.
[10] P.-G. De Gennes, P.-G. Gennes, Scaling concepts in polymer physics, Cornell university press, 1979.
[11] J.M. Urueña, et al., Mesh size control of polymer fluctuation lubrication in Gemini hydrogels, Biotribology 1–2 (2015) 24–29.
[12] J. Zhang, N.A. Peppas, Synthesis and characterization of pH- and temperature-sensitive Poly(methacrylic acid)/Poly(N-isopropylacrylamide) interpenetrating polymeric networks, Macromolecules 33 (1) (2000) 102–107.
[13] A.A. Pitenis, et al., Polymer fluctuation lubrication in hydrogel gemini interfaces, Soft Matter 10 (44) (2014) 8955–8962.
[14] N. Annabi, et al., Controlling the porosity and microarchitecture of hydrogels for tissue engineering, Tissue Eng. Part B, Reviews 16 (4) (2010) 371–383.
[15] K.D. Schulze, et al., Polymer osmotic pressure in hydrogel contact mechanics, Biotribology 11 (2017) 3–7.
[16] G.W. Scherer, Mechanics of syneresis I. Theory, J. Non-Cryst. Solids 108 (1) (1989) 18–27.
[17] G.W. Scherer, Mechanics of syneresis II. Experimental study, J. Non-Crystalline Solids 108 (1) (1989) 28–36.
[18] M. Rubinstein, R.H. Colby, Polymer physics, Vol. 23 Oxford University Press, New York, 2003.
[19] S. Kundu, A.J. Crosby, Cavitation and fracture behavior of polyacrylamide hydrogels, Soft Matter 5 (20) (2009) 3963–3968.
[20] W. Zhang, et al., Single polymer chain elongation of poly(N-isopropylacrylamide) and poly(acrylamide) by atomic force microscopy, J. Phys. Chem. B 104 (44) (2000) 10258–10264.
[21] D.A. Lucca, K. Herrmann, M.J. Klopfstein, Nanoindentation: measuring methods and applications, CIRP Ann. 59 (2) (2010) 803–819.
[22] D.C. Lin, E.K. Dimitriadis, F. Horkay, Elasticity of rubber-like materials measured by AFM nanoindentation, Express Polym Lett 1 (9) (2007) 576–584.